Critical Scaling of Granular Rheology

Takahiro HATANO

Earthquake Research Institute, University of Tokyo, Tokyo 113-0032, Japan

Rheology of dense granular matter in the vicinity of the jamming transition is investigated. Critical scaling laws that describe shear stress, pressure, and kinetic temperature are investigated. The scaling exponents are modified from those previously estimated by the present author [T. Hatano, J. Phys. Soc. Jpn. **77** (2008), 123002] and also compared with those proposed by Otsuki and Hayakawa [M. Otsuki and H. Hayakawa, Prog. Theor. Phys. **121** (2009), 647].

§1. Introduction

Granular matter is a conglomeration of macroscopic particles such as sand or cereals, the mass of which is so large that the thermal fluctuation is irrelevant to their motion. In general, the mechanical properties of granular matter seem almost unpredictable in the sense that granular matter often undergoes unexpected fluidization or solidification,[1] which typically results in a serious hazard (e.g. landslide, avalanche, or flow cessation in a silo). The mechanical properties of granular matter are thus important problems particularly in industrial societies and geosciences. Such sudden fluidization or solidification may be a reminiscence of thermodynamic phase transition.[2] However, the phenomenology of this "phase transition" has not been extracted until very recently. A breakthrough is brought about by Aharonov and Sparks,[3] who find that the rigidity transition is accompanied by discontinuous jump of the bulk modulus and the average coordination number, while the shear modulus are continuous. It is three years later that O'Hern et al.[4,5] rediscover the rigidity transition in a system of frictionless spheres. Due to the simplicity of this model, they can extract the critical nature of the rigidity transition using finite size scaling and some other scaling relations.

Quite interestingly, the rigidity transition also affects rheology of a dense granular matter.[6] A granular matter above the critical density acquires the yield stress. Critical scaling laws, which are of the same form as those in conventional critical phenomena, are found in the rheology of dense athermal systems near the critical density.[7,8] However, aside from numerical results and empirical laws, our understanding of granular rheology from the fundamental point of view is still very poor. The main difficulty in any statistical-mechanics approach is the dissipative nature of grains; there is no thermal equilibria regardless of the apparent similarity in some simple driven systems.[9] This means that conventional thermodynamics or equilibrium statistical mechanics do not apply. While a kinetic theory[10] can be applied to dense granular matter to a remarkable degree,[11] the applicability is limited to a nearly elastic system (i.e., the coefficient of restitution is close to 1.) In addition, kinetic theories generally involve binary collisions between hard spheres and thus cannot be applied to marginally rigid granular matter, in which the average coordi-

nation number reaches 6. Although one may be tempted to apply any theories that are useful in thermal systems (e.g., mode-coupling theory), we must first look into the phenomenon very carefully before the blind application of conventional theories.

Along the line of thought, numerical simulation on a simple model plays a considerable role in investigating rheology of athermal systems in order to extract phenomenology. Nevertheless, we still cannot theoretically derive (or explain) dense granular rheology obtained by simulation. The main difficulties are the strongly correlated motion of grains developed in dense systems.[12)–16)] Therefore, any microscopic (particle-based kinetic) theory for granular rheology must suitably incorporate this correlation, which is generally difficult even in a simple dilute gas.[17)] In this paper, we investigate the rheological properties of dense granular matter by numerical simulation in order to characterize their critical nature in terms of the rigidity transition.

§2. Model

We consider a bidisperse mixture of frictionless particles, the diameters of which are d and $0.7d$, respectively. The ratio of the numbers is 1 : 1. For simplicity, we assume that the mass of these particles are the same, which is denoted by M. The diameter and the position of particle i are denoted by R_i and $\boldsymbol{r}_i$, respectively. The force between particles i and j is written as $\boldsymbol{F}_{ij} = [k\delta_{ij} + \zeta \boldsymbol{n}_{ij} \cdot \dot{\boldsymbol{r}}_{ij}]\, \boldsymbol{n}_{ij}$, where $\boldsymbol{n}_{ij} = \boldsymbol{r}_{ij}/|\boldsymbol{r}_{ij}|$, $\boldsymbol{r}_{ij} = \boldsymbol{r}_i - \boldsymbol{r}_j$, and δ_{ij} denotes the overlap length, $(R_i + R_j) - |\boldsymbol{r}_{ij}|$. (Note that $\delta_{ij} = 0$ if $(R_i + R_j) < |\boldsymbol{r}_{ij}|$). Throughout this study, we adopt the units in which $d = 1$, $M = 1$, and $k = 1$. We adopt $\zeta = 0.1$, which corresponds to the coefficient of restitution being approximately 0.85.

In order to ensure uniform shear flow, we adopt the SLLOD equations[18)] together with the Lees-Edwards boundary conditions.[19)]

$$\dot{\boldsymbol{q}}_i = \frac{\boldsymbol{p}_i}{m_i} + \gamma q_{z,i} \boldsymbol{n}_y, \tag{2·1}$$

$$\dot{\boldsymbol{p}}_i = \sum_j \boldsymbol{F}_{\mathrm{ij}} - \gamma p_{z,i} \boldsymbol{n}_y, \tag{2·2}$$

where γ denotes the shear rate. The system is of constant volume and consists of 4000 particles. Here we investigate several volume densities ranging from 0.63 to 0.66. We discuss the rheological properties of this system with respect to two control parameters: the shear rate γ and the volume density ϕ. Note that the shear stress and the pressure are defined through the virial.[20)]

§3. Rheology and jamming

3.1. *Rheology*

First we investigate rheology of the present system at several densities near the critical density, above which granular matter acquires yield stress. As is shown in Fig. 1, the shear stress tends to a nonzero constant in the $\gamma \to 0$ limit for the density larger than 0.648. The critical density is thus located between 0.645 and 0.648 in

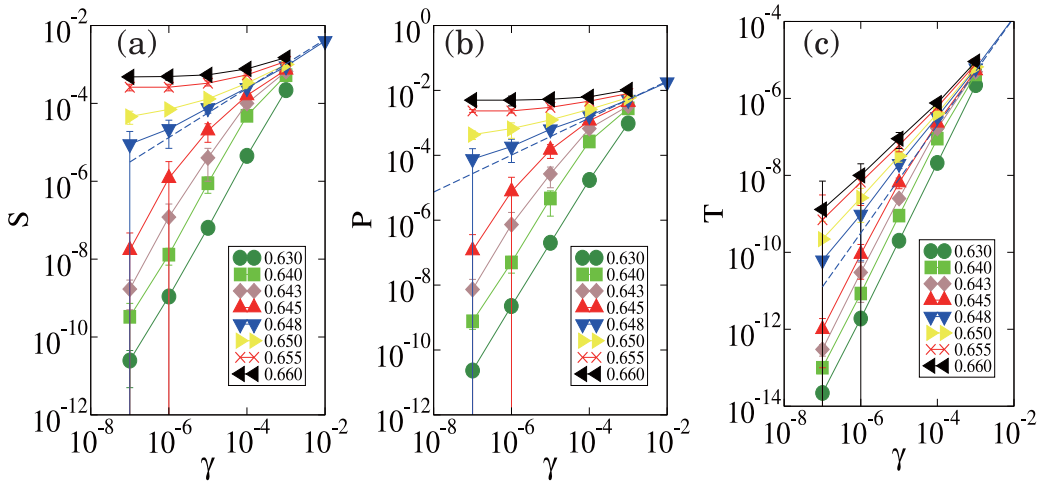

Fig. 1. (Color online) Granular rheology near the critical density. The data at the same density are linearly connected by the solid line, which is a guide for the eye. The error bars are the square root of the variance with respect to the temporal fluctuation; e.g., $\langle S(t)^2\rangle - \langle S(t)\rangle^2$. (a) Shear stress. The dashed line is proportional to $\gamma^{0.63}$. (b) Pressure. The dashed line is proportional to $\gamma^{0.57}$. (c) Kinetic temperature. The dashed line is proportional to $\gamma^{1.3}$.

the present system. Below the critical density, the shear stress S and the pressure P vanish in the $\gamma \to 0$ limit, obeying Bagnold's scaling,[21] $S \propto \gamma^2$ and $P \propto \gamma^2$. Note also that the kinetic temperature defined by $T = (3N)^{-1}\langle \sum_i \boldsymbol{p}_i^2 \rangle$ vanishes in the $\gamma \to 0$ limit irrespective of density.

3.2. *Estimate of the critical density*

In order to determine the critical density more precisely, we adopt the following protocol, which is similar to that utilized by O'Hern et al.[4),5)] (i) Prepare a system of given density ϕ, in which the grains are randomly distributed. (ii) Realize a steady state with shear rate $\gamma = \gamma_0$. (iii) Stop shear flow (let $\gamma = 0$) at $t = 0$ and let the system relax. (iv) Observe the relaxation of shear stress, $S(t)$. The system is jammed if the residual shear stress exists ($S(\infty) > 0$, as is shown in Fig. 2 (a)). (v) Iterate the above procedure using a different configuration of grains. The jamming probability is then obtained as a function of density, $P_J(\phi)$. Here we adopt $\gamma_0 = 10^{-2}$.

As the present system is rather small ($N = 4000$), $P_J(\phi)$ is a smooth function as is shown in Fig. 2(b), although it is expected to be a step function in the $N \to \infty$ limit. We define the critical density of the present system as the density at which the jamming probability is 0.5. By doing so, the critical density ϕ_J of the present binary system is estimated as $0.6472 < \phi_J < 0.6474$. Note that the critical density of the present system is apparently smaller than that for the infinite ($N \to \infty$) system, which is estimated as 0.648 using finite size scaling.[4)]

Interestingly, in the vicinity of the critical density, the decay of shear stress obeys a power law $t^{-\alpha}$, where $\alpha \simeq 0.7$. (See Fig. 2(a).) This power-law relaxation of shear stress is also observed in the relaxation process using overdamp dynamics, where $\alpha \simeq 0.5$.[22)]

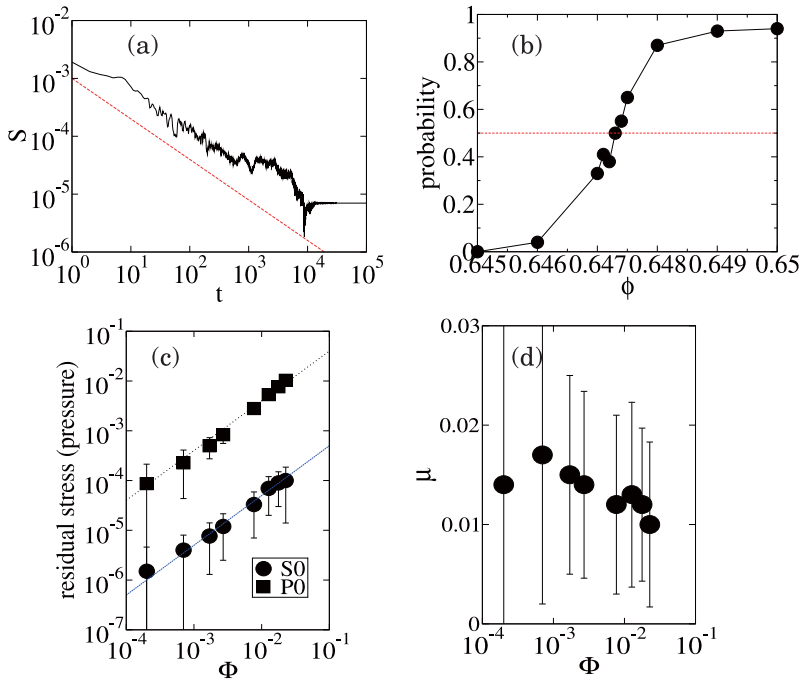

Fig. 2. (Color online) (a) Relaxation of shear stress after the flow cessation at $t = 0$. Shown is a jammed system, in which the shear stress eventually relaxes to a nonzero value. The dashed line is proportional to $t^{-0.7}$. (b) The jamming probability $P_J(\phi)$. See text for the definition. The dashed line is 0.5. The symbols are linearly connected by the solid line, which is a guide for the eye. (c) The residual shear stress (circles) and pressure (squares). (d) The residual friction coefficient. The error bars are the square root of the variance.

However, it should be remarked that the critical density determined in this manner seems to depend on the initial shear rate, γ_0, although the dependence is small.

3.3. *Residual shear stress*

Here we investigate further the properties of residual stress, which is a symptom of a jammed system. We define the averaged residual stress S_0 as $\langle S(\infty)\rangle$. This quantity increases as a function of density as is shown in Fig. 2(c), where the residual stress is proportional to the distance from the critical density, $S_0 \propto \Phi \equiv \phi - \phi_J$. Here we set $\phi_J = 0.6473$ based on the analysis in the previous subsection. As the shear modulus G is proportional to $\Phi^{0.5}$ for Hookean spring particles,[5] the residual strain, $\epsilon_0 = S_0/G$, is also proportional to $\Phi^{0.5}$. We can also define the averaged residual pressure $P_0 = \langle P(\infty)\rangle$, which is proportional to the density difference Φ as is shown in Fig. 2(c). Note that this behavior is also observed in an unsheared system.[5] Contrastingly, the averaged residual friction coefficient defined as $\mu_{\rm res} = \langle S(\infty)/P(\infty)\rangle$ is independent of the density as is shown in Fig. 2(d). It is important to notice that $\mu_{\rm res} \simeq 0.01$ is much smaller than the kinetic friction in the $\gamma \to 0$ limit, which is typically estimated as 0.06 or 0.1.[23),24)] Thus, the residual shear

stress should not be identified as the shear stress in the $\gamma \to 0$ limit, which is expected to exhibit a different behavior as is discussed in the next subsection.

3.4. *The quasistatic limit*

Here we show that the properties of shear stress and pressure in the $\gamma \to 0$ limit are apparently different from those of a static system ($\gamma = 0$). We simulate the quasistatic shear deformation by iterating the following procedure. i) A system undergoes instantaneous shear deformation with the applied strain being ϵ_0. ii) The system is relaxed to a local energy minimum using the conjugate gradient method. Iterating the above procedure for n times, the total strain ϵ applied to the system is $n\epsilon_0$. Then shear stress and pressure are represented as functions of strain, such as $S(\epsilon)$, $P(\epsilon)$. A typical behavior of $S(\epsilon)$ is shown in Fig. 3(a). Then we take the averaged stresses with respect to the strain. Here we adopt $S = n^{-1} \sum_{i=100}^{n+100} S(i\epsilon_0)$. Here we choose $n = 200$ and $\epsilon_0 = 0.001$. Note that we discard the data for $\epsilon < 0.1$.

The averaged stress and pressure as functions of density are shown in Fig. 3(b). Here we wish to stress that the shear stress and the pressure are proportional to $|\Phi|^{1.5}$, whereas the residual stress and pressure are proportional to $|\Phi|^{1.0}$ as is confirmed in the previous subsection. Note also that the friction coefficient is approximately 0.1, which is comparable to the results from extrapolation ($\gamma \to 0$) of the dynamic simulation.[23),24)] This indicates that the elastic properties of a marginally yielding system is different from those far from yielding. In terms of strain, the yield strain, $\epsilon_Y = S_0/G$, is proportional to $\Phi^{1.0}$, whereas the residual strain after the flow cessation is proportional to $\Phi^{0.5}$. However, at this point, we do not have any explanation for these scaling properties.

It should also be noted that the equivalence of this protocol for the quasistatic deformation to the vanishing shear rate limit with inertia is not trivial. We do not discuss further this problem in this paper.

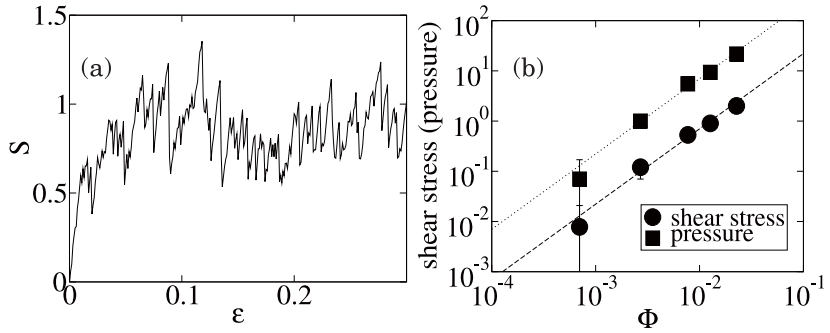

Fig. 3. (a) The behavior of shear stress as a function of strain in the quasistatic shear deformation. ($\gamma \to 0$). The density is 0.66. (b) The averaged shear stress and pressure in the $\gamma \to 0$ limit. The dashed and dotted lines are proportional to $|\Phi|^{1.5}$.

§4. Scaling properties

4.1. *Scaling laws*

Rheology of a dense granular matter obeys critical scaling of the following form,[8)]

$$S = |\Phi|^{y_\Phi} \mathcal{S}_\pm \left(\frac{\gamma}{|\Phi|^{y_\Phi / y_\gamma}} \right), \tag{4·1}$$

where $\mathcal{S}_\pm(\cdot)$ is a scaling function and Φ denotes $\phi - \phi_J$. Note that $\mathcal{S}_+$ and $\mathcal{S}_-$ correspond to $\Phi > 0$ and $\Phi < 0$, respectively. The data shown in Fig. 1(a) collapse using this scaling law with the exponents $y_\Phi = 1.5(1)$ and $y_\Phi / y_\gamma = 2.5(1)$, as is shown in Fig. 4(a). We set the critical density $\phi_J = 0.6473$, which is obtained in §3.2. By inseting $\gamma = 0$ into Eq. (4·1) and provided that $\mathcal{S}_+(0) \neq 0$, we obtain $S \propto |\Phi|^{1.5}$, which is consistent with the result obtained in §3.4.

The pressure and the kinetic temperature also obey scaling laws of the same

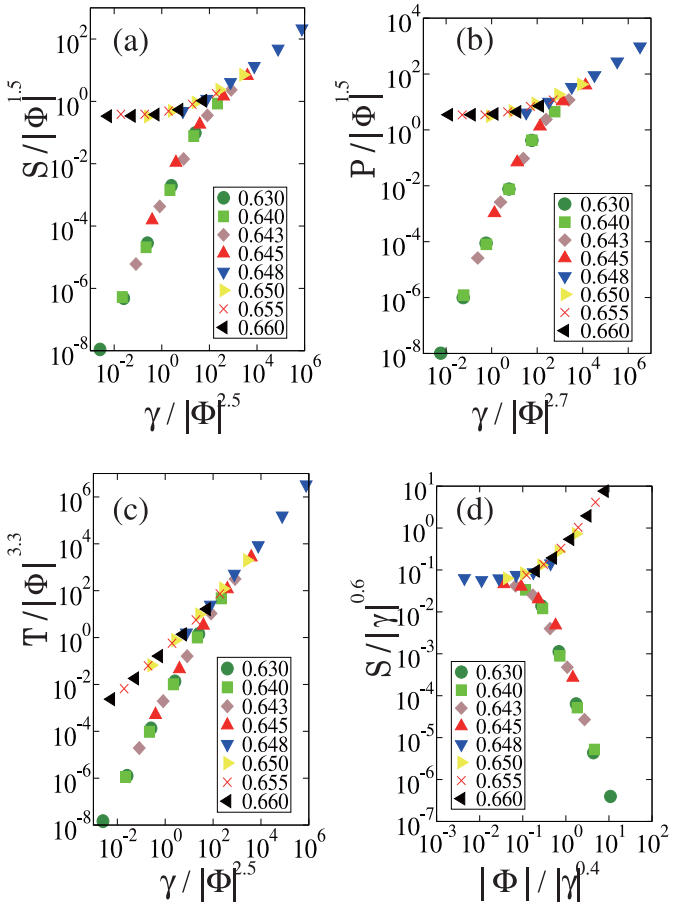

Fig. 4. (Color online) Critical scaling laws for mechanical properties: (a) Eq. (4·1) for shear stress, (b) Eq. (4·2) for pressure, (c) Eq. (4·3) for kinetic temperature, and (d) Eq. (4·4) for shear stress.

form as Eq. (4·1).

$$P = |\Phi|^{y'_\Phi} \mathcal{P}_\pm \left(\frac{\gamma}{|\Phi|^{y'_\Phi / y'_\gamma}} \right), \tag{4·2}$$

$$T = |\Phi|^{x_\Phi} \mathcal{T}_\pm \left(\frac{\gamma}{|\Phi|^{x_\Phi / x_\gamma}} \right), \tag{4·3}$$

as is shown in Figs. 4(b) and (c). Note that $y_\Phi / y_\gamma \simeq y'_\Phi / y'_\gamma \simeq x_\phi / x_\gamma \simeq 2.5$. These scaling laws imply that shear stress, pressure, and kinetic temperature are expressed as homogeneous functions of γ and Φ in the vicinity of the critical density. Furthermore, they are of the same form as those in conventional critical phenomena and thus may be due to the criticality of the jamming transition.

The exponents estimated here are slightly different from those previously estimated by the present author,[8] where the crossover exponent was 1.9(2), and $y_\Phi = y'_\Phi$ was 1.2(1). For several reasons, we believe that the exponents presented here are more precise than before: (i) The density range is closer to the critical density ($|\Phi| < 0.015$, while $|\Phi| < 0.15$ in the previous paper.) (ii) The precision of the critical density is improved by using a procedure independent of steady-state rheology. (iii) Shear rate is much lower ($10^{-7} \leq \gamma \leq 10^{-2}$) than before ($10^{-4} \leq \gamma \leq 10^{-1}$) in order to approach the critical point located at $\gamma = 0$ and $\phi = \phi_J$.

4.2. *Critical region*

The scaling law for shear stress, Eq. (4·1), can be rewritten as

$$S = |\gamma|^{y_\gamma} \mathcal{S}^* \left(\frac{\Phi}{|\gamma|^{y_\gamma / y_\Phi}} \right), \tag{4·4}$$

which predicts $S \propto |\gamma|^{y_\gamma}$ at the critical density ($\Phi = 0$). This relation can be used for the direct estimate of y_γ and thus important. In using Eq. (4·4), it is essential to notice that we cannot exactly set $\Phi = 0$ in numerical simulation because the critical density is not analytically obtained; i.e., the numerical error is inevitable in the estimated critical density. If a numerical value of ϕ_J contains $\pm\epsilon$ error, the critical rheology can be observed only where $\mathcal{S}^* \left(\pm\epsilon / |\gamma|^{y_\gamma / y_\Phi} \right) \simeq \mathcal{S}^*(0)$. The behavior of the scaling function $\mathcal{S}^*(x)$ is shown in Fig. 4(d). Note that $\mathcal{S}^*(x) \simeq \mathcal{S}^*(0)$ only where $|x| < 3 \times 10^{-2}$. Therefore, the region in which the critical rheology can be observed is

$$|\gamma| > (30\epsilon)^{y_\Phi / y_\gamma}. \tag{4·5}$$

We can quantitatively confirm the critical region, Eq. (4·5), together with Eq. (4·4). For example, as the critical density is estimated as $\phi_J = 0.6473(1)$ in §3.2, the numerical error is $\epsilon \simeq 1 \times 10^{-4}$. Then Eq. (4·5) leads to $|\gamma| > 5 \times 10^{-7}$. As is shown in Fig. 5(c), rheology at $\phi = 0.6473$ shows the critical behavior $S \propto \gamma^{y_\gamma}$ with $y_\gamma = 0.63(2)$ for $|\gamma| \geq 1 \times 10^{-6}$, whereas the deviation is apparent for $|\gamma| = 1 \times 10^{-7}$. Similarly, Eq. (4·5) predicts that the critical rheology can be observed only where $|\gamma| > 1 \times 10^{-4}$ at $\phi = 0.6480$ and 0.6466, as $\epsilon \simeq 7 \times 10^{-4}$. This behavior is also confirmed in Fig. 5(c).

§5. Discussion

5.1. *Comparison with other results*

We numerically estimate the exponents in a critical scaling law, Eq. (4·1); $y_\Phi = 1.5(1)$ and $y_\Phi/y_\gamma = 2.5(1)$. It should be noted that Otsuki and Hayakawa[31),32)] (OH) also investigate Eq. (4·1) to propose $y_\Phi = 1.0$ and $y_\Phi/y_\gamma = 2.5$. They compare this result with the previous result of the present author and concluded that the exponents[8)] was not precise because it is conducted in a parameter region away from the critical point. In the present paper, we thus set shear rate ($\gamma \geq 10^{-7}$) as low as theirs ($\gamma \geq 5 \times 10^{-7}$) with the system size being the same with theirs ($N = 4000$). As a result, we obtain $y_\Phi/y_\gamma \simeq 2.5$, which is consistent with that of OH. However, each exponent is still different: Here we estimate that $y_\Phi = 1.5(1)$ and $y_\gamma = 0.63(2)$, whereas OH conclude that $y_\Phi = 1.0$ and $y_\gamma = 0.4$.

In order to make a further comparison, we adopt only the data at lower shear rates ($10^{-7} \leq \gamma \leq 10^{-5}$), which is 20 percents smaller than theirs ($5 \times 10^{-7} \leq \gamma \leq 5 \times 10^{-5}$), to find that the data cannot collapse with the exponents proposed by OH. See Fig. 5(b). Note that OH use $\phi_J = 0.6480$ upon scaling collapse,[32)] which may be considered as the critical density in the $N \to \infty$ limit.[4)] We wish to remark that the critical density of a finite system ($\phi_J = 0.6473$ for $N = 4000$) is more appropriate for scaling of a finite system, otherwise the estimate of the exponents cannot be accurate due to finite size effect.

The error in critical density also affects the estimate of y_γ using Eq. (4·4). If we assume $\phi_J = 0.648$, the deviation from the true critical density, $\phi_J = 0.6473(1)$, is 7×10^{-4}. Then, from Eq. (4·5), the critical rheology ($S \propto \gamma^{y_\gamma}$) can be observed only where $|\gamma| > 1 \times 10^{-4}$. Because OH use $\gamma < 5 \times 10^{-5}$, they can never observe the true critical behavior. Although rheology for $\gamma \leq 10^{-4}$ seems to be consistent with their prediction $y_\gamma \simeq 0.4$, these data cannot be used for the estimate of y_γ as is

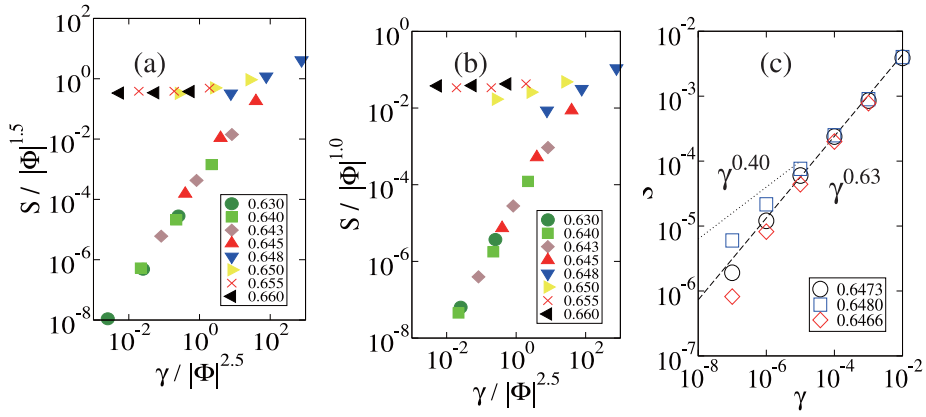

Fig. 5. (Color online) Critical scaling law for shear stress using only the data for lower shear rates ($10^{-7} \leq \gamma \leq 10^{-5}$). The critical density is set to be 0.6473. (a) Scaling collapse using the exponents estimated in the present paper. (b) Scaling collapse using the exponents estimated by Otsuki and Hayakawa. (c) Critical rheology and crossover. See text and Eq. (4·4).

explained above and in §4.2. it should be stressed that we can obtain $y_\gamma = 0.63$ in the critical region estimated with Eq. (4·5). It should also be remarked that $y_\gamma \simeq 0.63$ is obtained in a monodisperse system of much larger size.[16)]

The other exponent y_Φ involves the dynamic yield stress; i.e., $S(\Phi, \gamma) \to |\Phi|^{y_\Phi}$ in the $\gamma \to 0$ limit. OH proposed $y_\Phi = 1.0$ based on the facts that $P \propto \Phi^{1.0}$ in unsheared systems[4)] and that $S/P = \Phi^0$ in sheared systems.[23),24)] However, it is not so trivial that the pressure in an unsheared system and that in a very-slowly sheared system show the same behavior. Indeed, as we have seen in §3.4, they are different. Note also that Olsson and Teitel[7)] obtain $S(\Phi, \gamma) \to |\Phi|^{y_\Phi}$ with $y_\Phi = 1.2(1)$, and that Tighe et al. obtain $y_\Phi = 1.5$[33)] in model systems without inertia.

5.2. *Criticality of jamming*

Although the apparent similarity of the jamming transition to conventional critical phenomena, jamming does not involve spontaneous symmetry breaking. In this sense, there is no apparent *order* parameter for the jamming transition. Alternatively, the bulk modulus, which is the second order derivative of the internal energy, undergoes discontinuous change upon jamming. This may classify the jamming transition into a second-order phase transition with pressure being an order parameter, although the shear modulus exhibits continuous change. However, as pressure and shear stress do not show any long-wavelength fluctuation, a simple mean-field theory, which leads to $\xi \sim |\Phi|^{-0.5}$, does not apply to pressure or shear stress. It is remarkable that, in the jamming transition, long wavelength fluctuation can be detected only in purely dynamic quantities such as velocity[7),16)] or the particle displacement during a certain time lag.[13)–15)] This makes an essential contrast to conventional critical phenomena, where an order parameter itself exhibits long wavelength fluctuation. Mean-field theory for the jamming transition, which predicts the divergence of correlation length, must take this difference into account. The relation between the scaling laws and the correlation length has to be investigated further.

5.3. *Conclusion*

We investigate scaling laws describing the rheological properties of dense granular matter, Eqs. (4·1) – (4·3), which are of the same as those in conventional critical phenomena. These scaling laws imply that shear stress, pressure, and kinetic temperature are expressed as homogeneous functions of γ and Φ in the vicinity of the critical density, and thus may be due to the criticality of the jamming transition. The exponents in these scaling laws are modified from those previously obtained by the present author.[8)] The exponents are also compared with those obtained by Otsuki and Hayakawa.[31),32)] We find that the difference between them is due to the numerical error in the estimate of critical density. We show how the numerical error affects these exponents.

Acknowledgements

The author would like to thank all the participants in the first week of YKIS 2009, particularly Jim Jenkins for discussions on granular friction. The author also

appreciates discussions with Hisao Hayakawa and Michio Otsuki in the review process.

References

1) K. Abe, *The Woman in the Dunes* (Vintage International, New York, 2001).
2) P. G. de Gennes, Rev. Mod. Phys. **71** (1999), S374.
3) E. Aharonov and D. Sparks, Phys. Rev. E **60** (1999), 6890.
4) C. S. O'Hern, S. A. Langer, A. J. Liu and S. R. Nagel, Phys. Rev. Lett. **88** (2002), 075507.
5) C. S. O'Hern, L. E. Silbert, A. J. Liu and S. R. Nagel, Phys. Rev. E **68** (2003), 011306.
6) T. Hatano, M. Otsuki and S. Sasa, J. Phys. Soc. Jpn. **76** (2007), 023001.
7) P. Olsson and S. Teitel, Phys. Rev. Lett. **99** (2007), 178001.
8) T. Hatano, J. Phys. Soc. Jpn. **77** (2008), 123002.
9) F. Rouyer and N. Menon, Phys. Rev. Lett. **85** (2000), 3676.
10) V. Garzó and J. W. Dufty, Phys. Rev. E **59** (1999), 5895.
11) N. Mitarai and H. Nakanishi, Phys. Rev. E **75** (2007), 031305.
12) J. A. Drocco, M. B. Hastings, C. J. Olson-Reichhardt and C. Reichhardt, Phys. Rev. Lett. **95** (2005), 088001.
13) A. R. Abate and D. J. Durian, Phys. Rev. E **76** (2007), 021306.
14) A. S. Keys, A. R. Abate, S. C. Glotzer and D. J. Durian, Nature Phys. **3** (2007), 260.
15) F. Lechenault, O. Dauchot, G. Biroli and J.-P. Bouchaud, Europhys. Lett. **83** (2008), 46003.
16) T. Hatano, arXiv:0804.0477.
17) K. Kawasaki and I. Oppenheim, Phys. Rev. **136** (1964), A1519.
18) P. J. Davis and B. D. Todd, J. Chem. Phys. **124** (2006), 194103.
19) M. P. Allen and D. J. Tildesley, *Computer Simulation of Liquids* (Oxford University Press, New York, 1987).
20) D. N. Zubarev, *Nonequilibrium Statistical Thermodynamics* (Consultants Bureau, New York, 1974).
21) L. E. Silbert, D. Ertas, G. S. Grest, T. C. Halsey, D. Levine and S. J. Plimpton, Phys. Rev. E, **64** (2001), 051302.
22) T. Hatano, Phys. Rev. E **79** (2009), 050301(R).
23) T. Hatano, Phys. Rev. E **75** (2007), 060301(R).
24) P.-E. Peyneau and J.-N. Roux, Phys. Rev. E **78** (2008), 011307.
25) R. Brito and M. H. Ernst, Europhys. Lett. **43** (1998), 497.
26) S. B. Savage and K. Hutter, J. Fluid. Mech. **199** (1989), 177.
27) GDR MiDi, Eur. Phys. J. E **14** (2004), 341.
28) O. Pouliquen, C. Cassar, P. Jop, Y. Forterre and M. Nicolas, J. Stat. Mech. (2006), P07020.
29) P. Jop, Y. Forterre and O. Pouliquen, Nature **441** (2006), 727.
30) C. Cassar, M. Nicolas and O. Pouliquen, Phys. Fluid **11** (2005), 1956.
31) M. Otsuki and H. Hayakawa, Prog. Theor. Phys. **121** (2009), 647.
32) M. Otsuki and H. Hayakawa, Phys. Rev. E **80** (2009), 011308.
33) B. P. Tighe, E. Woldhuis, J. J. C. Remmers, W. van Saarloos and M. van Hecke, arXiv:1003.1268.